Arabian Journal of Chemical and Environmental Research
Vol. 12 Issue 2 (2025) 110–123

Wastewater Remediation by Adsorption Using Activated Carbon Prepared from Almond Residues Collected at the Federal Polytechnic Idah Premises

M. Husaini[1]*, Y. Danladi[1] and M. Hamza[1]

[1]*Department of Chemistry/Biochemistry, School of Technology, Federal Polytechnic Idah, Kogi State. P.M.B.1037, Nigeria*

Received 13 June 2025, Revised 20 Aug 2025, Accepted 23 Aug 2025

Cited as: *M. Husaini, Y. Danladi and M. Hamza (2025). Wastewater Remediation by Adsorption Using Activated Carbon Prepared from Almond Residues Collected at the Federal Polytechnic Idah Premises, Arab. J. Chem. Environ. Res. 12(2), 110-123*

Abstract
This study explores the effectiveness of activated carbon produced from almond residues collected within the Federal Polytechnic Idah premises for the removal of methyl orange dye from aqueous solutions. The prepared adsorbent was characterized using Scanning Electron Microscopy (SEM), Fourier Transform Infrared Spectroscopy (FTIR), Brunauer–Emmett–Teller (BET) surface area analysis, point of zero charge (pH_{pzc}), bulk density, and iodine number determination. SEM analysis revealed a porous surface structure favorable for adsorption, while FTIR confirmed the presence of hydroxyl, carboxyl, and other functional groups involved in dye interaction. BET analysis showed a high specific surface area, and the iodine number indicated strong adsorption potential. Batch adsorption experiments were conducted to assess the influence of contact time, initial dye concentration, adsorbent dosage, and pH. Kinetic modeling showed that the adsorption process followed a pseudo-second-order model, indicating chemisorption as the primary mechanism. The results demonstrate that almond-residue-based activated carbon is a cost-effective, environmentally friendly, and efficient material for the remediation of dye-contaminated wastewater.

Keywords: *Almond shell, Activated carbon, Methyl orange, Adsorption kinetics, Wastewater treatment*

**Corresponding author.*
E-mail address: musahusaini36@gmail.com

1. Introduction

Water pollution is one of the most pressing environmental challenges facing the modern world, particularly in developing regions where industrial and domestic effluents are often discharged into water bodies with minimal treatment (Lema, 2025; Lemessa *et al.*, 2023; Akartasse *et al.*, 2022). Among various pollutants, synthetic dyes, phenolic compounds, and heavy metals are especially hazardous due

ISSN : 2458-6544

to their toxicity, persistence, and resistance to biodegradation (Al-Hyali *et al.*, 2023; Husaini *et al.*, 2023a, Nairat *et al.*, 2022; Akartasse *et al.*, 2017). These contaminants not only affect aquatic life but also pose serious health risks to humans through contaminated drinking water and food chains. Therefore, effective and sustainable wastewater treatment methods are essential to ensure water safety and environmental protection (Chouli *et al.*, 2024, Azzaoui *et al.*, 2023).

Adsorption is widely regarded as one of the most efficient, economical, and eco-friendly methods for wastewater treatment. It offers significant advantages over conventional treatment technologies such as coagulation-flocculation, membrane filtration, or advanced oxidation, due to its simplicity, low energy requirements, and high selectivity for a wide range of contaminants (Ali *et al.*, 2023; Husaini *et al.*, 2024a, Er-rajy *et al.*, 2025, Alshahateet *et al.*, 2024). Activated carbon (AC), in particular, is one of the most effective adsorbents due to its high surface area, porous structure, and rich surface functional groups that facilitate strong interactions with pollutants (McCaffrey *et al.*, 2024; Husaini *et al.*, 2023b, Latifi *et al.*, 2025, Azzaoui *et al.*, 2024, Deghles *et al.*, 2019).

Traditionally, commercial activated carbon is derived from non-renewable sources such as coal or peat, which are expensive and environmentally unsustainable. In recent years, there has been growing interest in producing activated carbon from renewable agricultural wastes, including coconut shells, rice husks, sawdust, and various fruit shells (Ahmad and Aftab, 2024, El Hammari *et al.*, 2023). These precursors are abundant, inexpensive, and offer a sustainable solution to both waste management and water purification. Among these, almond shells have attracted attention due to their high lignocellulosic content, hardness, and carbon-rich structure, which make them excellent candidates for the production of high-quality activated carbon (Chen *et al.*, 2025; Husaini and Ibrahim, 2025).

This study aims to explore the conversion of almond shell residues collected at the Federal Polytechnic Idah premises into activated carbon, and to assess its efficiency in removing model pollutants such as methyl orange dye from aqueous solutions through the adsorption process. The adsorption data will be modeled using kinetic equations such as pseudo-first-order, and pseudo-second-order models. This study not only provides a low-cost solution to local water pollution issues but also promotes waste valorization, contributing to sustainable environmental management within the institution and beyond.

2. Materials and methods

2.1. Collection and Preparation of Raw Material

Almond residues (specifically almond seed shells) were collected within the Federal Polytechnic Idah premises. The raw materials were washed thoroughly with distilled water to eliminate surface impurities and then sun-dried for several days. The dried shells were further oven-dried at 105 °C for 24 hours to remove residual moisture.

2.2. Carbonization and Activation

The dried almond shells were ground to a fine powder and subjected to carbonization in a muffle furnace at 400 °C for 1 hour under limited oxygen supply. The resulting char was chemically activated by soaking it in 0.5 M phosphoric acid (H_3PO_4) in a 1:1 weight ratio. After impregnation, the sample was heated at 500 °C for 1 hour. The activated carbon was washed repeatedly with distilled water until neutral pH was attained, and then dried at 105 °C for 12 hours (Muhammad *et al.*, 2023).

2.3. Preparation of Methyl Orange Dye Solution

A stock solution of methyl orange dye (1000 mg/L) was prepared by dissolving an accurately weighed amount of dye in distilled water. Working solutions of varying concentrations (10–100 mg/L) were prepared by appropriate dilutions.

2.4. Characterization

Activated carbon was prepared from almond residues and characterized to determine its suitability for methyl orange adsorption. BET surface area and porosity were determined using nitrogen adsorption techniques. SEM was used to observe surface morphology and pore structure. FTIR analysis was performed to identify functional groups involved in dye binding. The pH at the point of zero charge (pH_{pzc}) was measured to assess surface charge behavior. Bulk density was determined by measuring the mass-to-volume ratio, and iodine number was used to evaluate micropore content. These methods collectively assessed the adsorbent's physical and chemical properties for effective dye removal.

2.5. Batch Adsorption Experiments.

Batch adsorption studies were conducted to investigate the removal efficiency of MO by AAC. The effect of various parameters such as contact time (10–180 min), initial dye concentration (10–100 mg/L), adsorbent dose (0.1–1.0 g), pH (2–10), and temperature (25–45 °C) were studied.Each experiment was carried out by adding a known amount of AAC into 100 mL of dye solution in a 250 mL conical flask (Abu Al-Rub *et al.*, 2024). The mixture was agitated at 150 rpm in an orbital shaker. After the predetermined contact time, the mixture was filtered, and the residual dye concentration was analyzed using a UV-Vis spectrophotometer at λ_{max}= 464 nm (Husaini *et al.*, 2024b).

2.6. Determination of Adsorption Parameters

The amount of dye adsorbed and the percentage removal efficiency were calculated using the equations:

$$Q_t = \frac{(C_0 - C_e) \times v}{m} \quad \textbf{1}$$

$$Q_e = \frac{(C_0 - C_e) \times v}{m} \qquad \textbf{2}$$

Where; C_0 and C_t are the initial and equilibrium concentrations of MB (mg/L), V is the volume of the solution (L), m is the mass of the adsorbent (g), Q_t and Q_e are the adsorption capacities at time *t* and at equilibrium (mg/g)

The percentage removal efficiency (%R) was also calculated as:

$$R\ (\%) = \frac{C_0 - C_e}{C_0} \times 100 \qquad \textbf{3}$$

3. Results and discussion

3.1 Characterization

3.1.1. SEM Analysis

SEM images presented in **Figure 1** revealed notable morphological changes from raw almond shell to activated carbon and after methyl orange adsorption. The raw material showed a smooth, compact surface with minimal porosity. After activation, the surface became rough and porous, indicating increased surface area suitable for adsorption. Following methyl orange adsorption, the pores appeared blocked and the surface smoother, confirming successful dye uptake by the activated carbon. These changes demonstrate the effectiveness of the activation process and the carbon's adsorption capacity.

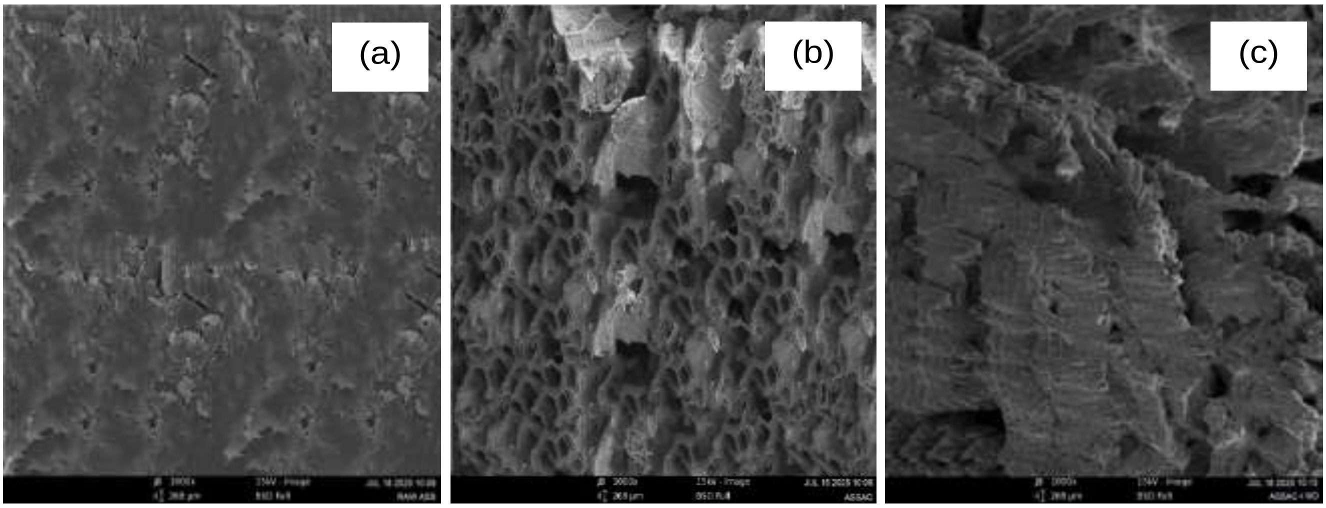

Figure 1. SEM Micrographs of Almond (a) Raw (b) Activated (b) After Adsorption

3.1.2. FT-IR Analysis

The FT-IR spectra (Figure 2) show chemical changes from raw almond shell to activated carbon and after methyl orange adsorption. Raw almond shell exhibited peaks at 3340 cm^{-1} (–OH), 2920 cm^{-1} (C–H), 1730 cm^{-1} (C=O), and 1040 cm^{-1} (C–O), indicating lignocellulosic structure (Tcheka *et al.*, 2024; El-Gendy and Younis, 2023). After activation, reduced C–H and C=O peaks and a new band at 1600

cm^{-1} (C=C) suggest decomposition of organics and formation of active sites (Desta and Lemma, 2023). Upon adsorption, shifts in –OH and C=O bands and appearance of a peak around 1500 cm^{-1} (N=N, C=C) confirm dye interaction. These spectral changes imply successful adsorption via hydrogen bonding, π–π interactions, and electrostatic attraction (Woldemariam and Alemayehu, 2024). The results confirm that surface functional groups played a key role in methyl orange uptake.

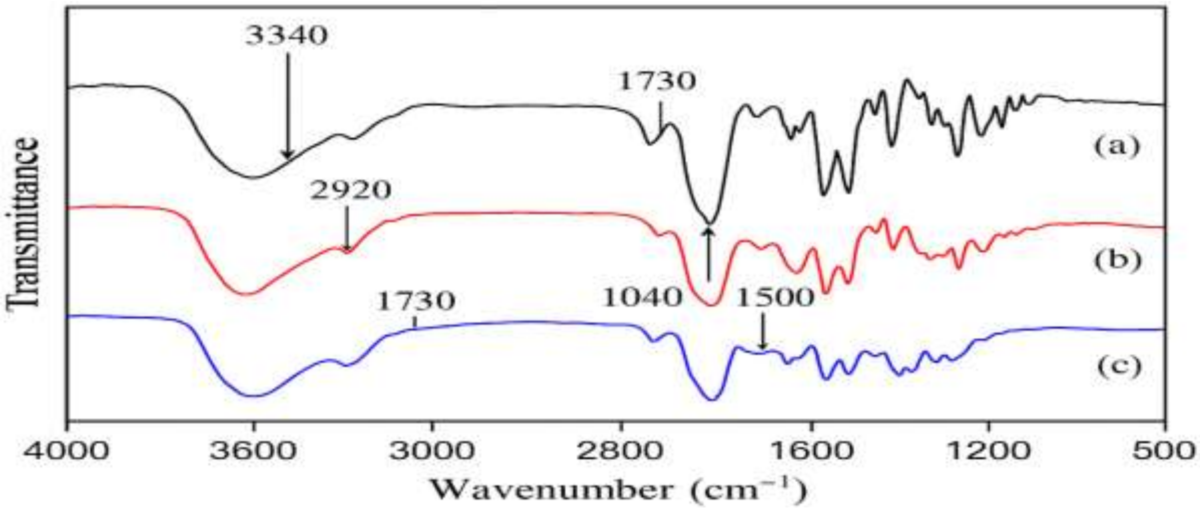

Figure 2: FTIR Spectra of (a) Raw Almond Shell (b) Activated Carbon (c) Activated Carbon after MO Adsorption

3.1.3. BET Analysis

The Brunauer–Emmett–Teller (BET) analysis was conducted to determine the surface area, pore volume, and pore size of the activated carbon prepared from almond residues (**Table 1**). These parameters are critical in evaluating the adsorptive capacity of the material for methyl orange removal (Hasan *et al.*, 2024; Mohamed and Salama 2022).

Table 1. BET Analysis Result

Parameter	Value	Unit
BET Surface Area (SBET)	823.45	m^2/g
Total Pore Volume (V_{total})	0.462	cm^3/g
Average Pore Diameter (D_{avg})	2.25	nm

The BET analysis reveals that the almond-residue-derived activated carbon possesses a high specific surface area of 823.45 m^2/g, indicating a significant availability of active sites for adsorption. The average pore diameter of 2.25 nm falls within the mesoporous range (2–50 nm), which is particularly favorable for adsorbing large dye molecules like methyl orange. The total pore volume of 0.462 cm^3/g also supports the potential for efficient diffusion and retention of dye molecules within the carbon matrix.

3.1.4. pH at Point of Zero Charge (ph_{pzc})

The point of zero charge (pH_{pzc}) of the prepared activated carbon was determined using the salt addition method to understand the surface charge characteristics of the adsorbent. The pH_{pzc} is defined as the pH at which the net surface charge of the activated carbon is zero (Tigrine *et al.,* 2024). At pH values below the pH_{pzc}, the surface of the adsorbent is positively charged, favoring the adsorption of anionic dyes such as methyl orange. Conversely, at pH values above the pH_{pzc}, the surface becomes negatively charged, which may repel the dye molecules due to electrostatic repulsion (Akinyeye and Adedeji, 2023).

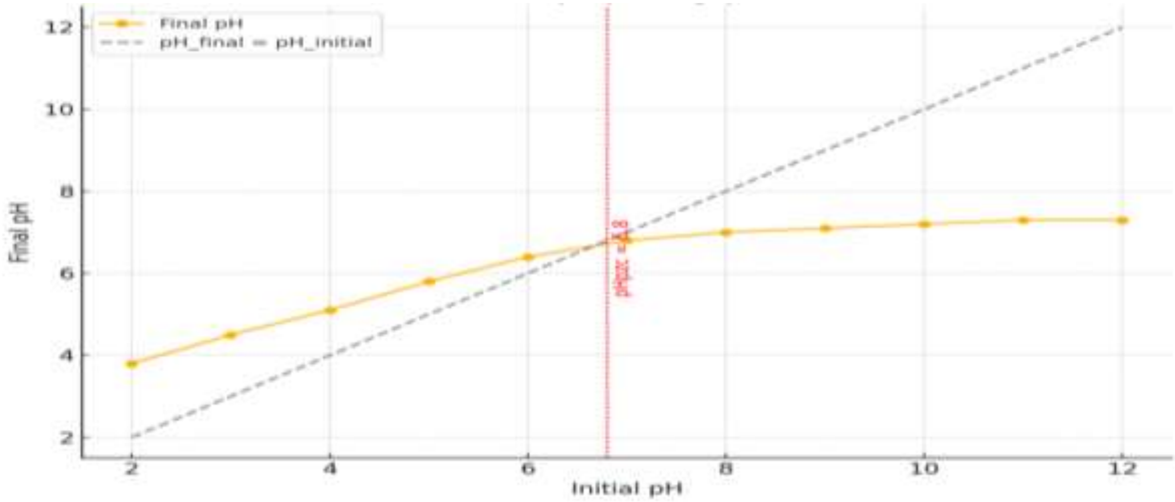

Figure 3. pH at Point of zero charge

The pH_{pzc} of the almond-based activated carbon was found to be approximately 6.8 (**Figure 3**) This indicates that the surface is positively charged under acidic to near-neutral conditions (pH < 6.8), which enhances the adsorption of methyl orange, an anionic dye. The result implies that the adsorption of methyl orange is favored in acidic conditions where electrostatic attraction dominates. This behavior aligns with the expected interaction between negatively charged dye molecules and the positively charged adsorbent surface at lower pH levels.

Therefore, knowledge of the pH_{pzc} is essential in optimizing the adsorption process, particularly when treating dye-laden wastewater under varying pH conditions.

3.1.5. Bulk Density and Iodine Number

The bulk density and iodine number are critical physicochemical parameters that influence the adsorption capacity of activated carbon. Bulk density reflects the compactness and porosity of the adsorbent, while the iodine number provides an estimate of the surface area and micropore content, especially useful in predicting its effectiveness in removing small molecular weight contaminants such as dyes (Farch *et al.,* 2024; Sahu *et al.,* 2025). The values obtained for the almond shell-based activated carbon (ASAC) are presented in **Table 2.**

Table 2. Bulk Density and Iodine Number

Parameter	Value	Unit	Method Used
Bulk Density	0.52	g/cm^3	Tapped density method
Iodine Number	843.75	mg/g	ASTM D4607-94

The bulk density of the prepared ASAC was found to be 0.52 g/cm^3, which falls within the acceptable range for powdered activated carbon (0.25–0.65 g/cm^3). A moderate bulk density suggests good packing and manageable flow properties, important for column applications (Chen *et al.*, 2025).

The iodine number was determined to be 843.75 mg/g, indicating a high surface area and microporosity. This value is comparable to that of commercial-grade activated carbon and suggests that ASAC is suitable for removing low molecular weight pollutants such as methyl orange. These properties imply that the prepared carbon has a high potential for adsorption of methyl orange, due to its adequate microporous structure and surface activity.

3.3 Adsorption Studies

The efficiency of activated carbon derived from almond residues in the adsorption of methyl orange dye from aqueous solution was investigated by varying key operational parameters as presented in Figure 4 (a-e).

From **Figure 4a,** the percentage removal of methyl orange increased steadily with time, reaching 76.0% at 60 minutes. A rapid increase was observed in the first 30 minutes, indicating the availability of abundant active sites on the adsorbent surface. After 40 minutes, the adsorption rate slowed and eventually plateaued, suggesting that the remaining active sites were less accessible due to repulsive forces between adsorbed dye molecules and the bulk solution (Farch *et al.*, 2024; Husaini *et al.*, 2023c). This behavior is typical of a two-stage process: an initial rapid surface adsorption followed by slower intraparticle diffusion. Equilibrium was essentially reached at 60 minutes, indicating that this is an optimal contact time for methyl orange removal using this adsorbent.

Figure 4b, illustrates that increasing the adsorbent dosage from 0.1 g to 1.0 g resulted in a higher percentage removal of methyl orange (from 19.0% to 86.4%). This can be attributed to the increase in surface area and the number of available adsorption sites as more adsorbent was introduced into the system. However, the adsorption capacity (q_e) decreased with increasing dosage. This inverse relationship is due to the unsaturation of adsorption sites at higher adsorbent dosages, as more sites are available than needed to accommodate the dye molecules present. This phenomenon also suggests some degree of particle aggregation at higher dosages, which reduces the effective surface area (Husaini *et al.*, 2023d).

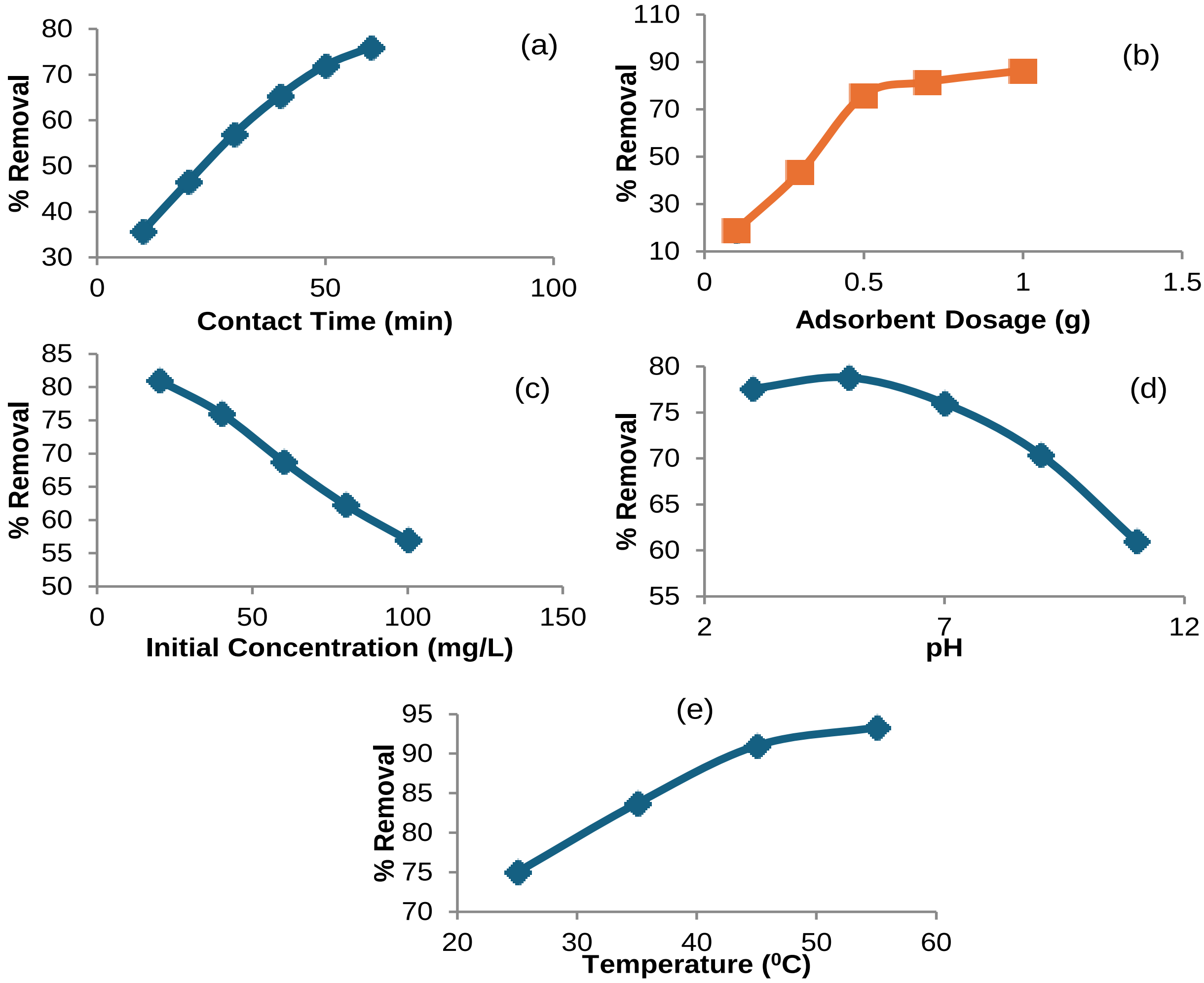

Figure 4. Effect of Various Experimental Parameters

As shown in **Figure 4c**, At low concentrations (20 mg/L), 81.0% of methyl orange was removed, corresponding to a q_e of 0.64 mg/g. At higher concentrations (100 mg/L), removal dropped to 57.0%, but the amount adsorbed per Gram of activated carbon increased to 5.70 mg/g. the adsorption capacity (q_e) increased with increasing initial dye concentration, while the percentage removal decreased. This trend occurs because higher initial dye concentrations provide a stronger driving force to overcome mass transfer resistance between the aqueous and solid phases. However, the fixed number of adsorption sites on the activated carbon becomes saturated at higher dye concentrations, leading to a reduced percentage removal (Husaini *et al.*, 2023e).

pH plays a crucial role in dye adsorption, particularly for anionic dyes like methyl orange. From **Figure 4d,** it is evident that maximum adsorption occurred in the acidic pH range (pH 3–5), with a peak removal of 78.8% at pH 5. As the pH increased beyond 7, the removal efficiency decreased, dropping to 61.0% at pH 11. This behavior can be explained by electrostatic interactions. In acidic solutions, the surface of activated carbon becomes positively charged, which enhances the electrostatic attraction with the negatively charged sulfonate groups of methyl orange. At higher pH levels, the surface charge becomes more negative due to deprotonation, leading to electrostatic repulsion between the adsorbent and the anionic dye, thereby reducing adsorption (Husaini *et al.*, 2023f).

Temperature plays a vital role in the adsorption process as it affects the mobility of dye molecules and the affinity of the adsorbent surface for the adsorbate. Figure 4e shows that the removal efficiency increased with temperature, suggesting an endothermic nature of the adsorption process. This may be due to enhanced dye diffusion into the pores of the activated carbon at higher temperatures and the generation of additional active sites on the adsorbent surface. The increase in adsorption capacity with temperature supports the assumption of increased interaction between the dye molecules and the activated carbon surface. This behavior is consistent with chemisorption, which is often associated with stronger interactions and energy uptake (Rabiu *et al.*, 2023; Husaini, 2024).

3.4 Adsorption Kinetics

To evaluate the mechanism and rate of methyl orange adsorption onto the prepared activated carbon, the experimental data were fitted to two widely used kinetic models: the pseudo-first-order and pseudo-second-order models. The results are presented in the Table 3.

Table 3: Kinetic Parameters for the Adsorption of Adsorbates by BPAC

Kinetic Model	Parameters	Values
Pseudo-first order	$k_1(min^{-1})$	0.047
	$q_{e\ exp}$ (mg/g)	3.60
	$q_{e\ cal}$ (mg/g)	3.82
	R^2	0.961
Pseudo-second order	K_2 (g/ mg min)	0.017
	$q_{e\ exp}$ (mg/g)	3.80
	$q_{e\ cal}$ (mg/g)	3.82
	R^2	0.997

3.4.1 Pseudo-First-Order Kinetics

The pseudo-first-order model assumes that the rate of occupation of adsorption sites is proportional to the number of unoccupied sites (Hii, 2021).

$$\ln (q_e - q_t) = \ln q_e - k_1 t \qquad 4$$

The linear form was applied using the experimental data from the time-dependent adsorption study. As shown in Table 3, the calculated rate constant (k_1) was 0.047 min^{-1}, and the correlation coefficient (R^2) was 0.961**.**

Although the model gave a reasonable fit (**Figure 5a**), there was a noticeable deviation between the experimental equilibrium adsorption capacity ($q_{e,exp}$ = 3.6 mg/g) and the calculated value ($q_{e,cal}$ = 3.82

mg/g). This suggests that while some adsorption occurs through physisorption processes, the pseudo-first-order model does not fully describe the adsorption mechanism.

3.4.2 Pseudo-Second-Order Kinetics

The pseudo-second-order model assumes that adsorption follows a chemisorption mechanism involving valency forces through sharing or exchange of electrons (Cordova *et al.*, 2021).

$$\frac{t}{q_t} = \frac{1}{k_2 q_e^2} + \frac{t}{q_e} \qquad 5$$

The linear form provided an excellent fit (**Figure 5b**) to the experimental data. The rate constant (k_2) was found to be 0.017 g/mg·min**,** and the correlation coefficient (R^2) was 0.997, which is significantly higher than that of the pseudo-first-order model. Additionally, the calculated q_e value (3.80 mg/g) was nearly identical to the experimental value, confirming the model's suitability.

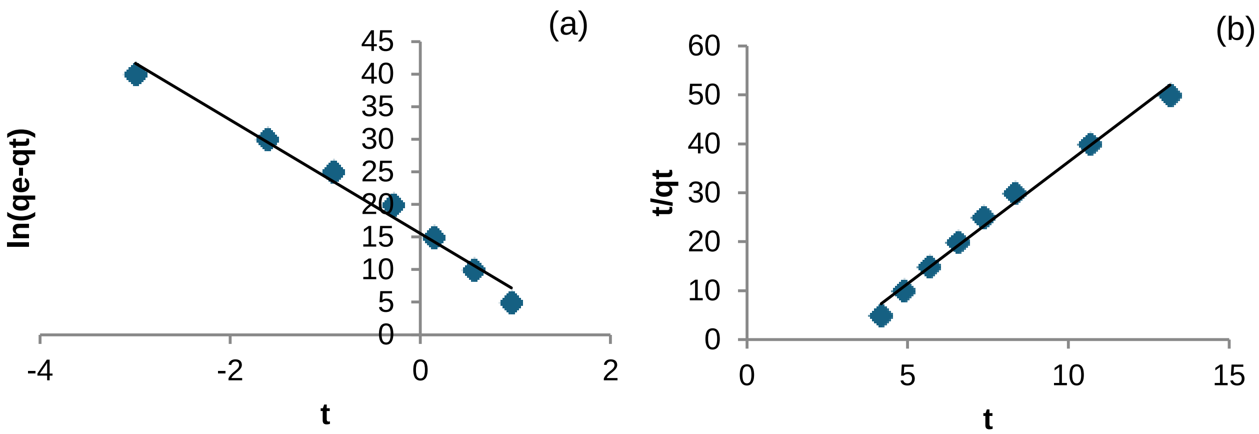

Figure 5: Plot for (a) Pseudo-first order (b) Pseudo-second order

The high R^2 value and good agreement of q_e values suggest that chemisorption is the dominant rate-limiting step in the adsorption of methyl orange onto almond-based activated carbon. This likely involves electrostatic interactions and possibly hydrogen bonding between the functional groups on the adsorbent surface and the dye molecules. Therefore, the methyl orange adsorption process onto the almond residue-based activated carbon follows pseudo-second-order kinetics**,** indicating that chemical interactions between the dye and the surface-active sites are more significant than simple physical adsorption.

Conclusion

The findings of this study confirm that activated carbon derived from almond residues is an effective adsorbent for the removal of methyl orange dye from aqueous solutions. The material exhibited excellent adsorption characteristics, as supported by surface morphology, functional group analysis, and textural properties. The adsorption process was strongly influenced by pH, contact time, and initial dye concentration, with optimal performance occurring in slightly acidic conditions (around pH 5–6). Kinetic analysis revealed that the adsorption followed a pseudo-second-order model, suggesting that the process was governed primarily by chemical interactions between the dye and the surface functional groups of the carbon. The high iodine number and BET surface area also support its strong adsorption capacity. Overall, the use of almond-based activated carbon offers a sustainable and low-cost approach to treating dye-laden wastewater, contributing to circular waste utilization and environmental protection.

Acknowledgement

The authors sincerely acknowledge the Tertiary Education Trust Fund (TETFUND) for their financial support, which made this research possible. The grant provided by TETFUND facilitated the procurement of materials, access to laboratory facilities, and characterization analyses necessary for the successful completion of this project.

Conflict of Interest

The authors declare that the research was conducted in the absence of any commercial or financial relationships that could be construed as a potential conflict of interest.

References

Abu Al-Rub, S. S., Alyami, B. A., Alqahtani, Y. S., Alqarih, A. R., Dunquwah, B. A., Alyami, M. M., … Alghithan, S. K. (2024). Comparative adsorption of methyl orange color from an aqueous solution using activated carbon. *Indian Journal of Pharmaceutical Education and Research,* 58 (2), 679–684. https://doi.org/10.5530/ijper.58.2.76

Ahmad, A., and Aftab, A. (2024). Green technology approach towards the removal of heavy metals, dyes, and phenols from water using agro-based adsorbents: A review. *Chemistry – An Asian Journal*. https://doi.org/10.1002/asia.202400154b

Akartasse , N., Mejdoubi, E., et al. (2017). Natural product based composite for extraction of arsenic (III) from waste water. *Chem Cent J.* 12; 11(1): 33. doi: 10.1186/s13065-017-0261-9.

Akartasse N., Azzaoui K., Mejdoubi E., Elansari L. L., *et al*. (2022), Chitosan-Hydroxyapatite Bio-Based Composite in film form: synthesis and application in Wastewater, *Polymers,* 14(20), 4265, https://doi.org/10.3390/polym14204265

Akinyeye, R. O., and Adedeji, A. A. (2023). Optimization and kinetic studies of methyl orange dye adsorption onto modified agricultural waste. *Scientific African*, 19, e01536. https://doi.org/10.1016/j.sciaf.2023.e01536

Al-Hyali, R. H., Al-Qazzaz, W. A., and Altamer, D. H. (2023). Adsorptive elimination of methyl orange dye over activated carbon derived from bitter almond shells: An isothermal, thermodynamic, and kinetic study. *Journal of the Turkish Chemical Society A: Chemistry*, *10*(2), 339–358. https://doi.org/10.18596/jotcsa.1177543

Ali, K., Zeidan, H., and Ben Amar, R. (2023). Evaluation of the use of agricultural waste materials as low-cost and eco-friendly sorbents to remove dyes from water: A review. *Desalination and Water Treatment*, *302*, 231–252. https://doi.org/10.5004/dwt.2023.29725

Altun, T., Ecevit, H., and Kar, Y. (2021). Adsorption of Cr(VI) onto cross-linked chitosan–almond shell biochars: Equilibrium, kinetic, and thermodynamic studies. *Journal of Analytical Science and Technology*, *12*, 38. https://doi.org/10.1186/s40543-021-00288-0

Azzaoui, K., Aaddouz, M., Akartasse, N. *et al.* (2024). Synthesis of β-Tricalcium Phosphate/PEG 6000 Composite by Novel Dissolution/Precipitation Method: Optimization of the Adsorption Process Using a Factorial Design—DFT and Molecular Dynamic. *Arab J Sci Eng* **49**, 711–732. https://doi.org/10.1007/s13369-023-08390-8

Azzaoui, K., Jodeh, S. et al. (2023). Synthesis of hydroxyapatite/polyethylene glycol 6000 composites by novel dissolution/ precipitation method: optimization of the adsorption process using a factorial design: DFT and molecular dynamic. *BMC Chemistry*, 17, 150 https://doi.org/10.1186/s13065-023-01061-7

Alshahateet, S. F., Al-Trawneh, S. A., Er-rajy, M., Zerrouk, M., Azzaoui, K., Al-Tawarh, W. M., Hammouti, B., Salghi, R., Sabbahi, R., Alanazi, M. M., & Rhazi, L. (2024). Green Synthesis of Zinc Oxide Nanoparticles for Tetracycline Adsorption: Experimental Insights and DFT Study. *Plants*, *13*(23), 3386. https://doi.org/10.3390/plants13233386

Chen, Y., Wang, D., Wang, X., et al. (2025). Enhanced adsorption of phenol using EDTA-4Na- and KOH-modified almond shell biochar. *Sustainable Environment Research*, *35*(1), Article 4. https://doi.org/10.1186/s42834-025-00243-3

Chen, Z., Zhang, C., Liu, F., and Zhao, Y. (2025). Preparation of KOH and EDTA-modified almond shell biochar and its application for phenol adsorption. *Sustainable Environment Research*, 35(1), Article 12. https://doi.org/10.1186/s42834-025-00243-3

Cordova, A. K. E., Lozano, F. C., and Díaz, R. A. L. (2021). Thermodynamics and kinetic studies for the adsorption process of methyl orange by magnetic activated carbons. *Industrial and Engineering Chemistry Research*, *60*(13), 4875–4884. https://doi.org/10.1021/acs.iecr.0c04925

Desta, M., and Lemma, B. (2023). Anchote peel as a low-cost biosorbent for the removal of methyl orange dye from aqueous solution: Characterization and adsorption studies. *Applied Water Science*, 13, 84. https://doi.org/10.1007/s13201-022-01832-y

Deghles, A., Hamed, O., Aza, M., Abu Lail, B., et al. (2019). Cellulose with bidentate chelating functionality: An adsorbent for metal ions from wastewater. *BioRes.* 14(3), 6247-6266.

El Hammari, L., Hamed, R., et al. (2023). Optimization of the adsorption of lead (II) by hydroxyapatite using a factorial design: Density functional theory and molecular dynamics. *Front. Environ. Sci.* 11:1112019. doi: 10.3389/fenvs.2023.1112019

El-Gendy, A., and Younis, N. (2023). Mesoporous activated wheat straw biochar for methyl orange removal: Surface chemistry and FTIR evidence. *ACS Sustainable Resource Management*, 2(4), 130–143. https://doi.org/10.1021/acssusresmgt.3c00109

Er-rajy, M., Salghi, R., Elhallaoui M., Azzaoui K. et al. (2025). Exploring donor-acceptor characteristics and adsorption behavior of a naphthamide-based inhibitor for protective surfaces through a molecular modeling approach. *Journal of the Indian Chemical Society*. 102, 4, 101640. https://doi.org/10.1016/j.jics.2025.101640

Farch, M., Bentahar, S., and Benaïssa, H. (2024). Comparative study of almond shell raw activated carbon, chemically activated and adsorption of anionic dye from wastewater. In *Proceedings of the 7th International Conference on Advances in Mechanical Engineering* (pp. 250–258). AIJR Publisher. https://books.aijr.org/index.php/press/catalog/book/170/chapter/3221

Hasan, A., Şahin, M., and Atay, F. (2024). Adsorptive elimination of methyl orange dye over bitter almond shell derived activated carbon. *Journal of the Turkish Chemical Society, Section A: Chemistry, 11*(2), 249–259. https://doi.org/10.18596/jotcsa.1177543

Hii, H. T. (2021). Adsorption isotherm and kinetic models for removal of methyl orange and Remazol Brilliant Blue R by coconut shell activated carbon. *Tropical Aquatic and Soil Pollution, 1*(1), 1–10. https://doi.org/10.53623/tasp.v1i1.4

Husaini M. (2024) Role of Organic Compound as Corrosion Inhibitor for Aluminium in Acidic Solution, *Arab. J. Chem. Environ. Res.*, 11(2), 95–109.

Husaini M., Usman B. and Ibrahim M. B. (2023a). Adsorption Studies of Methylene Blue using Activated Carbon Derived from Sweet Detar Seed Shell, *ChemSearch J.*, 14(1), 21–32.

Husaini M., Usman B. and Ibrahim M. B. (2023b). Combined Computational and Experimental Studies for the Removal of Anionic Dyes using Activated Carbon Derived from Agricultural Waste, *Appl. J. Environ. Eng. Sci.*, 9(4), 245–258.

Husaini M., Usman B. and Ibrahim M. B. (2023c). Competitive Adsorption of Congo Red Dye from Aqueous Solution onto Activated Carbon Derived from Black Plum Seed Shell in Single and Multicomponent System, *Afr. J. Manag. Eng. Technol.*, 1(2), 76–89.

Husaini M., Usman B. and Ibrahim M. B. (2023d). Kinetic and Thermodynamic Evaluation on Removal of Anionic Dye from Aqueous Solution using Activated Carbon Derived from Agricultural Waste: Equilibrium and Reusability Studies, *Appl. J. Environ. Eng. Sci.*, 9, 124–138.

Husaini M., Usman B. and Ibrahim M. B. (2023e). Modeling and Equilibrium Studies for the Adsorption of Congo Red Using *Detarium microcarpum* Seed Shell Activated Carbon, Appl. J. Environ. Eng. Sci., 9, 147–162.

Husaini M., Usman B. and Ibrahim M. B. (2023f). Thermodynamic and Equilibrium Evaluation for Anionic Dye Adsorption using Utilized Biomass-based Activated Carbon: Regeneration and Reusability Studies, *Arab. J. Chem. Environ. Res.*, 10(1), 1–116.

Husaini M., Usman B. and Ibrahim M. B. (2024a). Biosorption of Methyl Orange Dye in Single, Binary and Ternary Systems onto Gingerbread Plum Seed Shell Activated Carbon, *J. Turk. Chem. Soc., Sec. A: Chem.*, 11(2), 655–664.

Husaini M., Usman B. and Ibrahim M. B. (2024b). Experimental and Quantum Chemical Evaluation for Methylene Blue Adsorption onto Activated Carbon, *Afr. J. Manag. Eng. Technol.*, 2(1), 51–62.

Husaini, M. and Ibrahim, M. B. (2025). Adsorption of cationic and anionic dyes in single and binary adsorption of cationic and anionic dyes onto activated carbon derived from agricultural waste. *J. Mater. Environ. Sci.*, 16(5), 881-893.

Latifi, M., Azzaoui, K, et al. (2025). Gum Arabic modified nano-hydroxyapatite for cobalt(II) removal from water: Adsorption performance and molecular-level mechanism. *Desalination and Water Treatment*. 323, 101272. https://doi.org/10.1016/j.dwt.2025.101272

Lema, M.W. (2025). Wastewater crisis in East African cities: challenges and emerging opportunities. *Discov Environ.*, 3, 18, https://doi.org/10.1007/s44274-025-00206-w

Lemessa F., Simane B., Seyoum A., Gebresenbet G. (2023). Assessment of the Impact of Industrial Wastewater on the Water Quality of Rivers around the Bole Lemi Industrial Park (BLIP), Ethiopia. *Sustainability.* 15(5), 4290. https://doi.org/10.3390/su15054290

McCaffrey, Z., Torres, L. F., Chiou, B. S., et al. (2024). Almond and walnut shell activated carbon for methylene blue adsorption. *ACS Sustainable Resource Management, 1*(7), 1421–1431.

https://doi.org/10.1021/acssusresmgt.4c00080

Mohamed, R. M., and Salama, M. (2022). Efficient adsorption of methyl orange on nanoporous carbon from *Moringa oleifera* seed waste. *Materials Proceedings, 6*(12), 385. https://doi.org/10.3390/materproc2022006385

Muhammad, S., Yahya, E. B., Abdul Khalil, H. P. S., Marwan, M., and Albadn, Y. M. (2023). Recent advances in carbon and activated carbon nanostructured aerogels prepared from agricultural wastes for wastewater treatment applications. *Agriculture, 13*(1), 208. https://doi.org/10.3390/agriculture13010208

Nairat, N., Hamed, O., Berisha, A. *et al.* (2022). Cellulose polymers with β-amino ester pendant group: design, synthesis, molecular docking and application in adsorption of toxic metals from wastewater. *BMC Chemistry* **16**, 43. https://doi.org/10.1186/s13065-022-00837-7

Rabiu, M. A., Husaini, M., Usman, B., Ibrahim, M. B. (2023). Adsorption of Basic Magenta Dye From Aqueous Solution Using Raw And Acid Modified Yam Peel As Adsorbent. *Bayero Journal of Pure and Applied Sciences*. 14(1), 460 – 466.

Sahu, S. K., Das, P., and Dash, B. (2025). Removal of Cr(VI) from aqueous solution using activated carbon derived from almond, peach, and apricot shell blends: Kinetic, isotherm and thermodynamic studies. *Water, Air, and Soil Pollution*, 236(4), 7910. https://doi.org/10.1007/s11270-025-07910-6

Tcheka, C., Zhang, W., Li, Y., and Mbemi, J. (2024). Valorization of date palm spikelets into activated carbon composite for enhanced methyl orange adsorption. *Environmental Science and Pollution Research*, 31, 13721–13735. https://doi.org/10.1007/s11356-024-34581-3

Tigrine, Z., Benhabiles, O., Merabti, L., Chekir, N., Mellal, M., Aoudj, S., Amele Abdeslam, N., Tassalit, D., and Lebouachera, S. E. I. (2024). Sustainable activated carbon from agricultural waste: A study on adsorption efficiency for humic acid and methyl orange dyes. *Sustainability*, 16(21), 9308. https://doi.org/10.3390/su16219308

Woldemariam, F. T., and Alemayehu, E. (2024). Sustainable activated carbons from agricultural wastes for water purification: A critical review. *Sustainability*, 16(21), 9308. https://doi.org/10.3390/su16219308